Vietnam Journal of Mechanics, VAST, Vol. 30, No. 1 (2008), pp. 55 – 66

STATIC AND DYNAMIC ANALYSIS OF LAMINATED COMPOSITE PLATES WITH INTEGRATED PIEZOELECTRICS

Tran Ich Thinh
Hanoi University of Technology
Le Kim Ngoc
Vietnam Electricity

Abstract. A Finite Element model based on First-order Shear Deformation Theory is developed for the static shape control and vibration control of laminated composite plates integrated with piezoelectric sensors and actuators. A nine-node isoparametric rectangular element with 45 degrees of freedom for the generalized displacements and 2 electrical degrees of freedom is implemented for the static and dynamic analyses. The model is validated by comparing with existing results documented in the literature. Some numerical results are presented. It is concluded that the shape of the piezoelectric laminated composite plates can reach the desired shape through passive control or active control. The influence of stacking sequence of composite plates and position of piezoelectric layers and sensors/actuators patches on the response of the piezoelectric composite plates is evaluated.

1. INTRODUCTION

Two basic phenomena characteristic piezoelectric materials and permit their use as sensors and actuators in intelligent structures. Piezoelectric materials can generate an electric charge when deformed, a property called the *direct piezoelectric effect.* The *converse piezoelectric effect* occurs when an electric field acts on a piezoelectric material to generate mechanical stresses and strains within the material [1] [2].

Based on these phenomena, in the recent years, there has been an increase in the developments of the laminated composite plates integrated with piezoelectric materials. The composite structures are bonded or embedded with piezoelectric materials in thin layers can greatly enhance the performance of existing structures such as sensory, adapting with static or dynamic responses as well as many application such as the shape control, nanopositioning, precision mechanics, active vibration suppression ...etc.

Several analysis and numerical models have been developed to analyze the laminated composite plates with integrated piezoelectric sensors and actuators. The often used model is the equivalent single layer model, which includes the Classical Plate Theory (CPT) [3], [7], [9] or First-order Shear Deformation Theory (FSDT) [4], [10] or High-order Shear Deformation Theory (HSDT) [5], [8]. For thick laminated composites structures, [6] show that Layerwise Theory has some advantages.

José, Cristóvão and Carlos [7] analyzed geometrically nonlinear of the composite plates/shells with integrated piezoelectric layers. The authors have chosen a nonconforming triangular plate element with 18 degree of freedom (DOF) for the generalized displacements and one DOF for the electricpotential.

Fukunaga, Hu and Ren [8] analyzed the static and dynamic problems of composite plates with integrated piezoelectric layers via penalty functions. In their analysis, a nine-noded nonconforming plate element with 5 DOF at each node and 1 DOF for each piezoelectric layer/patch.

Liu, Peng and Lam [9] studied the dynamic response of the composite plates with piezoelectric layers using a four-node rectangular nonconforming plate element.

Liu, Dai and Lim [10] used meshless method to calculate the static and dynamic behaviour of the piezolaminated composite plates.

In the present paper, we used a nine-noded isoparametric element with 45 DOF and 2 electric potential DOF based on FSDT to investigate the static behaviour of the composite plates integrated piezoelectric layers. The effect ofstacking sequence and position of piezoelectric layers on deflection of composite plate is examined. The influence of sensor/actuator patches position on the dynamic responses of the laminated plates is evaluated.

2. DISPLACEMENT AND STRAIN FIELDS

The laminated composite plate integrated on upper/lower surface with piezoelectric is considered. It is assumed that the piezoelectric layers are perfectly bonded. The displacement field is expressed by:

$$\begin{aligned} u(x,y,z,t) &= u_0(x,y,t) + z\theta_x(x,y,t), \\ v(x,y,z,t) &= v_0(x,y,t) + z\theta_y(x,y,t), \\ w(x,y,z,t) &= w_0(x,y,t), \end{aligned} \tag{1}$$

where, u_0, v_0 and w_0 are the displacement components of a point on the midplane in the x, y and z directions, t is the time variable and θ_x and θ_y are the rotations of normals to the midplane about the y and x axes, respectively.

Expressing the displacement field in terms of shape functions $(N_i(\xi,\eta))$ and element nodal displacements, gives:

$$\{u(\xi,\eta)\} = \sum_{i=1}^{n} N_i(\xi,\eta).\,\{u\}_i\,, \tag{2}$$

n is the element node number; ξ, η are the natural co-ordinates.

The electric potential is constant over the element surface:

$$\phi_k\,(\xi,\eta) = \sum_{i=1}^{n} N_i(\xi,\eta)\phi_i. \tag{3}$$

A voltage ϕ applied across an actuator of layer thickness t generates an electric field vector $\{E\}$, such that:

$$\begin{aligned} E_k &= -\nabla\phi_k = \{\ 0 \quad 0 \quad E_k^z\ \} \\ E_k^z &= -\phi_k/t_k = [B_\phi]\{\phi\} = \begin{bmatrix} 0 & 0 & \frac{1}{t_{p1}} & 0 & 0 & 0 \\ 0 & 0 & 0 & 0 & 0 & \frac{1}{t_{p2}} \end{bmatrix}^T \begin{bmatrix} \phi_1 \\ \phi_2 \end{bmatrix}, \end{aligned} \tag{4}$$

where t_k is the thickness of the k^{th} piezoelectric layer.

Applying FSDT, the strain-displacement relationship becomes:

$$\{\varepsilon\} = \begin{bmatrix} \varepsilon_x^M \\ \varepsilon_y^M \\ \gamma_{xy}^M \\ \varepsilon_x^B \\ \varepsilon_y^B \\ \varepsilon_{xy}^B \\ \gamma_{yz} \\ \gamma_{xz} \end{bmatrix} = \begin{bmatrix} \frac{\partial}{\partial x} & 0 & 0 & 0 & 0 \\ 0 & \frac{\partial}{\partial y} & 0 & 0 & 0 \\ \frac{\partial}{\partial y} & \frac{\partial}{\partial x} & 0 & 0 & 0 \\ 0 & 0 & 0 & z\frac{\partial}{\partial x} & 0 \\ 0 & 0 & 0 & 0 & z\frac{\partial}{\partial y} \\ 0 & 0 & 0 & z\frac{\partial}{\partial y} & z\frac{\partial}{\partial x} \\ 0 & 0 & \frac{\partial}{\partial y} & 0 & 1 \\ 0 & 0 & \frac{\partial}{\partial x} & 1 & 0 \end{bmatrix} \begin{bmatrix} u \\ v \\ \mathrm{w} \\ \theta_y \\ \theta_x \end{bmatrix} \tag{5}$$

$$= [\partial] \begin{bmatrix} u \\ v \\ w \\ \theta_y \\ \theta_x \end{bmatrix} = [\partial]\,[N]\,\{u\}_i = [B_u]\,\{u\}_i\,.$$

According to [7], [8], [9], [11], [12] the linear piezoelectric constitutive equations coupling the elastic and electric fields take the form:

$$\boldsymbol{\sigma} = \boldsymbol{Q}\boldsymbol{\varepsilon} - \boldsymbol{e}\boldsymbol{E}, \tag{6}$$

$$\boldsymbol{D}^p = \boldsymbol{e}^T\boldsymbol{\varepsilon} + \boldsymbol{p}\boldsymbol{E}, \tag{7}$$

in which $\boldsymbol{\sigma} = \{\sigma_x\ ,\ \sigma_y\ ,\ \tau_{xy}\ ,\ \tau_{yz}\ ,\ \tau_{xz}\}^T$ is the elastic stress vector

$\boldsymbol{\varepsilon} = \{\varepsilon_x\ ,\ \varepsilon_y\ ,\ \gamma_{xy}\ ,\ \gamma_{yz}\ ,\ \gamma_{xz}\}^T$: elastic strain vector;

$\boldsymbol{Q}$ is the element stiffness matrix;

$\boldsymbol{E}$: electric field vector;

$\boldsymbol{D}^p$: electric displacements vector;

$\boldsymbol{e}$: piezoelectric stress coefficients matrix;

$\boldsymbol{p}$: permittivity coefficients matrix.

3. CONSTITUTIVE EQUATIONS COUPLING THE PIEZOELECTRIC EFFECT

The membrane $\{N\}$, bending $\{M\}$ and shear $\{Q\}$ stress resultants are the integrals of the stress components. From (6) and (7), we obtain the constitutive equations in matrix form:

$$\begin{Bmatrix} \{N\} \\ \{M\} \\ \{Q\} \\ \{D_1^p\} \\ \{D_2^p\} \end{Bmatrix} = \begin{bmatrix} [A] & [B] & 0 & [e]_1 & [e]_2 \\ [B] & [D] & 0 & [e]_1 & [e]_2 \\ 0 & 0 & [F] & 0 & 0 \\ [e]_1 & [e]_1 & 0 & [p]_1 & 0 \\ [e]_2 & [e]_2 & 0 & 0 & [p]_2 \end{bmatrix} \begin{Bmatrix} \varepsilon^M \\ \varepsilon^B \\ \gamma \\ -E_1 \\ -E_2 \end{Bmatrix} \tag{8}$$

$(^M)$, $(^B)$ are the membrane and bending components respectively.

$(^p)$ is the piezoelectric layer. Subscripts $(_1)$, $(_2)$ denote the k^{th} piezoelectric layer.

$$[A] = [A_{ij}]$$

$$[A_{ij}]_{3\times 3} = \sum_{k=1}^{n} (h_k - h_{k-1}) \left(Q'_{ij}\right)_k + \sum_{k=1}^{m} (h_k - h_{k-1}) \left(Q_{ij}\right)_k \quad i,j = 1,2,6$$

$$[B] = [B_{ij}]$$

$$[B_{ij}]_{3\times 3} = \frac{1}{2}\sum_{k=1}^{n} \left(h_k^2 - h_{k-1}^2\right) \left(Q'_{ij}\right)_k + \frac{1}{2}\sum_{k=1}^{m} \left(h_k^2 - h_{k-1}^2\right) \left(Q_{ij}\right)_k \quad i,j = 1,2,6$$

$$[D] = [D_{ij}]$$

$$[D_{ij}]_{3\times 3} = \frac{1}{3}\sum_{k=1}^{n} \left(h_k^3 - h_{k-1}^3\right) \left(Q'_{ij}\right)_k + \frac{1}{3}\sum_{k=1}^{m} \left(h_k^3 - h_{k-1}^3\right) \left(Q_{ij}\right)_k \quad i,j = 1,2,6$$

$$[F] = [F_{ij}]$$

$$[F]_{2\times 2} = \sum_{k=1}^{n} f\,(h_k - h_{k-1}) \left(Q'_{ij}\right)_k + \sum_{k=1}^{m} f\,(h_k - h_{k-1}) \left(Q_{ij}\right)_k f = 5/6;\ i,j = 4,5$$

n and m are the respective numbers of composite and piezoelectric layers. $[Q'_{ij}]$ is the reduced stiffness matrix [13].

$$[H]_{8\times 8} = \begin{bmatrix} [A]_{3\times 3} & [B]_{3\times 3} & [0]_{3\times 2} \\ [B]_{3\times 3} & [D]_{3\times 3} & [0]_{3\times 2} \\ [0]_{2\times 3} & [0]_{2\times 3} & [F]_{2\times 2} \end{bmatrix}_{8\times 8}.$$

4. FINITE ELEMENT EQUATIONS

4.1. Static analyses

Finite element equations take the form [14]:

$$\begin{bmatrix} K_{uu} & K_{u\phi} \\ K_{\phi u} & K_{\phi\phi} \end{bmatrix} \begin{Bmatrix} u \\ \phi \end{Bmatrix} = \begin{Bmatrix} F_u \\ Q_\phi \end{Bmatrix}, \tag{9}$$

F_u and Q_ϕ are respectively the applied external load and charge

4.2. Dynamic analyses

From Hamilton's principle [9], we have

$$\delta \int_{t_1}^{t_2} [T - U + W]dt = 0, \tag{10}$$

$$T^e = \frac{1}{2}\int_{V_e} \rho \{\dot{u}\}^T \{\dot{u}\}\, dV_e, \tag{11}$$

$$U^e = \frac{1}{2}\int_{V_e} \{\varepsilon\}^T \{\sigma\} dV_e, \tag{12}$$

$$W^e = \int_{V_e} \{u\}^T \{f_b\} dV_e + \int_{S_e} \{u\}^T \{f_s\}\, dS_e + \{u\}^T \{f_c\}, \tag{13}$$

T and U are respectively the kinetic and potential energy and W, the work done by external forces. *fb*, *fs* and *fc* are respectively the body, surface and concentrated forces acting on the plate. S_e and V_e are elemental area and volume.

Substitute Eqs. (1), (2), (3), (4), (5), (10), (11) and (12) into (9) using (6) and (7), to obtain:

$$M_{uu}\ddot{u} + K_{uu}u + K_{u\phi}\phi = F, \tag{14}$$

$$K_{\phi u}u - K_{\phi\phi}\phi = Q. \tag{15}$$

Substitute (15) into (14) to obtain:

$$M_{uu}\ddot{u} + \left(K_{uu} + K_{u\phi}K_{\phi\phi}^{-1}K_{\phi u}\right)u = F + K_{u\phi}K_{\phi\phi}^{-1}Q. \tag{16}$$

4.3. Free vibration

In (16), set the external load F and charge Q to zero to describe free vibration.

$$M_{uu}\ddot{u} + \left(K_{uu} + K_{u\phi}K_{\phi\phi}^{-1}K_{\phi u}\right)u = 0. \tag{17}$$

Plate vibrations induce charges and electric potentials in sensor layers. The control system allows a current to flow and feeds this back to the actuators. If we apply no external charge Q to a sensor, we have from (9) and (15).

$$\phi_s = \left[K_{\phi\phi}^{-1}\right]_s [K_{\phi u}]_s u_s. \tag{18}$$

$$Q_s = [K_{\phi u}]_s u_s \text{is the induced charge due to deformation.} \tag{19}$$

The operation of the amplified control loop implies the actuating voltage is:

$$\phi_a = G_d\phi_s + G_v\dot{\phi}_s, \tag{20}$$

G_d and G_v are respectively the feedback control gains for displacement and velocity

From (15), the charge in the actuator due to actuator deformation in response to plate vibration modified by control system feedback is:

$$Q_a = [K_{\phi u}]_a u_a - [K_{\phi\phi}]_a \left(G_d\phi_s + G_V\dot{\phi}_s\right). \tag{21}$$

Substitute (18) into (21) to yield:

$$[K_{\phi u}]_a u_a - G_d [K_{\phi\phi}]_a \left[K_{\phi\phi}^{-1}\right]_s [K_{\phi u}]_s u_s - G_V [K_{\phi\phi}]_a \left[K_{\phi\phi}^{-1}\right]_s [K_{\phi u}]_s \dot{u}_s = Q_a. \tag{22}$$

Substitute (22) into (16) and incorporate structural damping to yield:

$$\begin{aligned} M_{uu}\ddot{u} + \left(K_{uu} + K_{u\phi}K_{\phi\phi}^{-1}K_{\phi u}\right)u &= F + K_{u\phi}K_{\phi\phi}^{-1}\left([K_{u\phi}]_a u_a\right. \\ &\left.-G_d [K_{\phi\phi}]_a \left[K_{\phi\phi}^{-1}\right]_s [K_{\phi u}]_s u_s - G_V [K_{\phi\phi}]_a \left[K_{\phi\phi}^{-1}\right]_s [K_{\phi u}]_s \dot{u}_s\right), \end{aligned} \tag{23}$$

where $u_s \equiv u_a \equiv u$ is the plate displacement vector $[K_{u\phi}]_a \equiv [K_{u\phi}]_s \equiv [K_{u\phi}]$ and $[K_{\phi\phi}]_a \equiv [K_{\phi\phi}]_s \equiv [K_{\phi\phi}]$ are respectively the mechanical-electrical coupling and piezo-electric permittivity stiffness matrices.

$$\begin{aligned} &M_{uu}\ddot{u} + \left(G_V [K_{\phi\phi}]_a \left[K_{\phi\phi}^{-1}\right]_s [K_{\phi u}]_s + \alpha M_{uu} + \beta K_{uu}\right)\dot{u} \\ &+ \left(K_{uu} + G_d [K_{\phi\phi}]_a \left[K_{\phi\phi}^{-1}\right]_s [K_{\phi u}]_s\right)u = F. \end{aligned} \tag{24}$$

Condensing the equations yields:

$$M_{uu}\ddot{u} + (C_A + C_R)\,\dot{u} + K^* u = F. \tag{25}$$

Set F to zero in (25) to obtain damped and undamped natural frequencies and mode shapes.

$$M_{uu}\ddot{u} + (C_A + C_R)\,\dot{u} + K^* u = 0, \tag{26}$$

$C_A = G_v\,[K_{u\phi}]_a \left[K_{\phi\phi}^{-1}\right]_s [K_{\phi u}]_s$: active Damping matrix
$C_R = \alpha M_{uu} + \beta K_{uu} \alpha = 0.5; \quad \beta = 0.25$
$K^* = [K_{uu}] + G_d\,[K_{u\phi}]_s \left[K_{\phi\phi}^{-1}\right]_s [K_{\phi u}]_s$: structural Damping matrix
$(_a)$, $(_s)$ subscripts denote respectively actuator and sensor

4.4. Matrices

Mass Matrix

$$M_{uu} = \int\limits_V \rho\,[N]^T\,[N]\,dV. \tag{27}$$

Mechanical Stiffness

$$[K_{uu}] = \int\limits_S [B_u]^T\,[H]\,[B_u]dS. \tag{28}$$

Mechanical-Electrical coupling

$$[K_{u\phi}] = \int\limits_S [B_u]^T\,[\bar{e}]\,[B_\phi]dS. \tag{29}$$

Electrical-Mechanical coupling

$$[K_{\phi u}] = [K_{u\phi}]^T. \tag{30}$$

Piezoelectric permittivity

$$[K_{\phi\phi}] = -\int\limits_S [B_\phi]^T\,[\bar{p}]\,[B_\phi]dS, \tag{31}$$

where $[B_\phi]$ and $[B_u]$ are defined in (4), and (5) and:

$$[\bar{e}]_{8\times6} = \begin{bmatrix} [e]_{1_{3\times3}} & [e]_{2_{3\times3}} \\ [e]_{1_{3\times3}} & [e]_{2_{3\times3}} \\ [0]_{2\times3} & [0]_{2\times3} \end{bmatrix} \qquad [\bar{p}]_{6\times6} = \begin{bmatrix} t_{p_1}\,[p]_{1_{3\times3}} & [0]_{3\times3} \\ [0]_{3\times3} & t_{p_2}\,[p]_{2_{3\times3}} \end{bmatrix}.$$

5. CASES STUDIES AND DISCUSSION

5.1. Static deflection control

Based on the presented algorithm, we find the numerical results. In the static control, all the piezoelectric layers on the uper and lower surfaces of the composite plate are used as actuators to change centerline deflection of the plate.

Consider a square plate ($a \times b = 0.2$ m$\times$0.2 m), only the b side is clamped (Fig. 1), six layers [p/-45^0/45^0/-45^0/45^0/p]. p is piezoelectric layer (PZT G1195N), the thickness of each piezoelectric layer is 0.1 mm. The composite layers are made of T300/976 graphite-epoxy, the thickness of each layer is 0.25 mm. Material properties are given in Table 1.

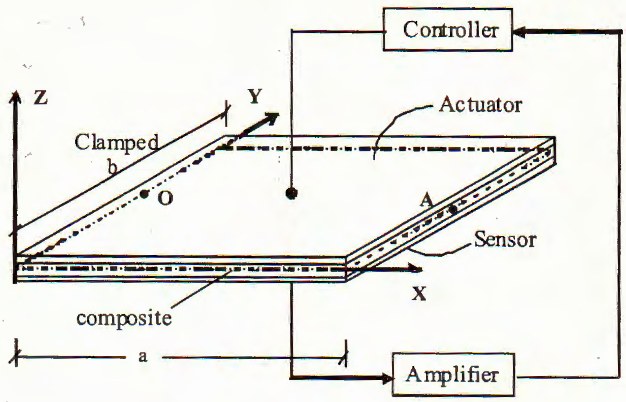

Fig. 1. Composite plate with integrated piezoelectric sensors and actuators, and feedback control.

Table 1. Material properties of PZT G1195N and T300/976

Material ID	E_{11} (GPa)	$E_{22}=E_{33}$ (GPa)	$\nu_{12}=\nu_{13}$ $\nu_{13}=\nu_{23}$	$G_{12}=G_{13}$ (GPa)	G_{23} (GPa)	ρ (kg/m^3)	$d_{31}=d_{32}$ (m/V)	$p_{11}=p_{22}$ (F/m)	p_{33} (F/m)
PZT G1195N	63.0	63.0	0.3	24.2	24.2	7600	254x10^{-12}	15.3x10^{-9}	15x10^{-9}
T300/976	150.0	9.0	0.3	7.1	2.5	1600	-	-	-

Case (1) Fig. 2 plots plate centerline deflection under 10 V actuator input voltage in the absence of an applied load. The plate bend up or down depending on the sign of the applied voltage.

Case (2) The plate is originally flat and is then exposed to a uniformly distributed load of 100 N/m^2. To flatten the plate, we apply a active voltage and it is added incrementally until the centerline deflection of the plate is reduced to a desired tolerance (*passive control*). Fig. 3 show these through OA centerline deflection when the plate under uniform loading and different level actuator input voltage.

Fig. 3 illustrates active deflection control for various actuator input voltages to limit the measured centerline deflection of an antisymmetric plate to desired tolerance.

Case (3) Consider a simply supported antisymmetric plate: $v_0 = w_0 = \theta_y = 0$ at $x = 0$, $x = a$; $u_0 = w_0 = \theta_x = 0$ at $y = 0$, $y = b$. Material properties are listed in Table 1.

Apply feedback gains $G_d = 0$, 20, 28 and 50 to the control system to limit static deflection (*active control*). When $G_d = 28$ volts, the plate is fully restored to shape and level.

Numerical results generated by a 5×5 element agree well with those Liu, Dai and Lim [10] obtained using mesh free techniques assuming 15×15 nodes.

5.2. Influence of ply angle and piezoelectric layer location

Using the plate illustrated in Fig. 1, compare the response of an antisymmetric laminate, [p/-θ^0/θ^0]$_{as}$, with symmetric laminate, [p/-θ^0/θ^0]$_s$, for actuator input voltages of 0

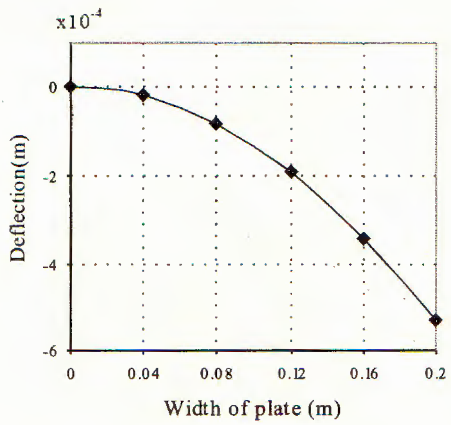

Fig. 2. Centerline deflection of the cantilever laminate [p/-45^0/45^0] as for an actuator input voltage of 10 Volt

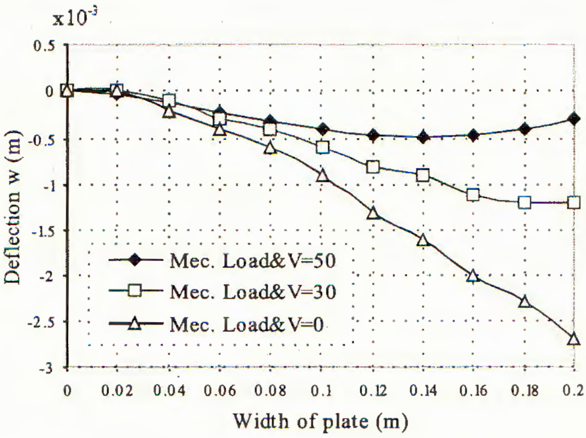

Fig. 3. Centerline deflection of the cantilever laminate [p/-45^0/45^0] as under uniform loading versus actuator input voltage

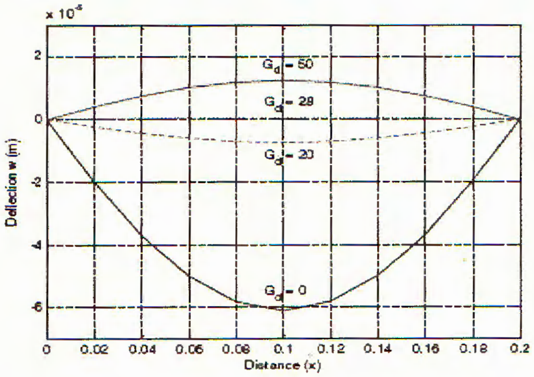

Fig. 4. The effect of displacement feedback control gain Gd on the static deflection of the simply supported laminate [p/-45^0/45^0]$_{as}$ under a uniform pressure load

V, 5 V and 10 V. Assume simple supports and plates carry a uniform 100 N/m^2 pressure load.

Table 2 lists results selectively illustrated in Fig. 5. The antisymmetric plate deflects more than the symmetric plate. An applied voltage of 10 V restores both plates to near level.

Results agree well with similar findings published in [10].

Table 2 and Fig. 5 taken together illustrate a slight decrease in plate bending stiffness with decreasing ply angle when V = 0.

5.3. Influence of sensor/actuator patch location

To exercise effective vibration control it is normal to use closed feedback control loops and install sensors and actuators as sensor/actuator pairs. Fig. 6 illustrates four configurations A, B, C and D being four pairs of of PZT G1195 N piezoelectric sensors and actuators bonded onto the top and bottom surfaces of a composite plate.

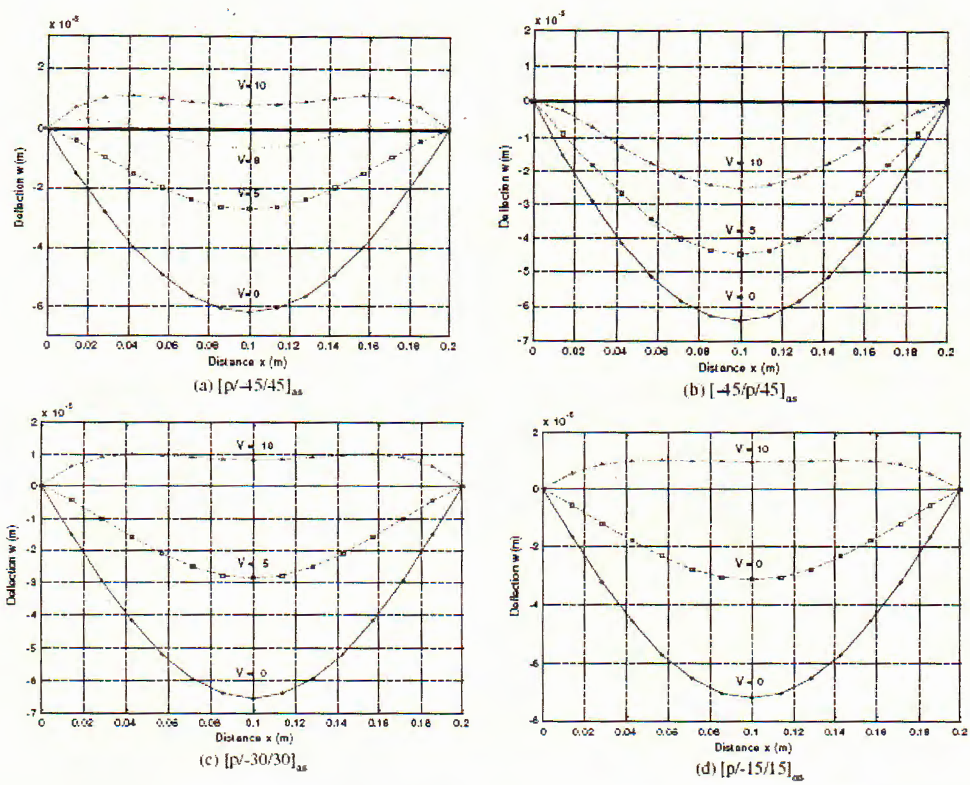

Fig. 5. Centerline deflection of a uniformly loaded simply supported laminated plate versus actuator input voltage

Table 2. Central node deflection (x 10^{-5} m) of simply supported laminates carrying a 100 N/m^2 uniform pressure load versus actuator input voltage. Dis. indicates the Discrepancy

Plate		Actuator input voltage								
		0 V			5 V			10 V		
		[10]	Present	Dis.	[10]	Present	Dis.	[10]	Present	Dis.
1	$[p/\text{-}45^0/45^0]_s$	-6.038	-5.724	5.2%	-2.717	-2.766	1.77%	0.604	0.585	3.15%
2	$[\text{-}45^0/p/45^0]_s$	-6.380	-6.388	0.13%	-4.570	-4.59	0.44%	-2.760	-2.79	1.08%
3	$[p/\text{-}45^0/45^0]_{as}$	-6.217	-6.220	0.05%	-2.73	-2.76	1.09%	0.757	0.739	2.38%
4	$[\text{-}45^0/p/45^0]_{as}$	-6.424	-6.430	0.09%	-4.480	-4.51	0.67%	-2.536	-2.58	1.71%
5	$[p/\text{-}30^0/30^0]_{as}$	-6.542	-6.570	0.43%	-2.862	-2.876	0.49%	0.819	0.819	0.01%
6	$[p/\text{-}15^0/15^0]_{as}$	-7.222	-7.276	0.74%	-3.134	-3.135	0.03%	0.954	0.961	0.69%

Consider a simply supported square plate [-30^0/30^0]$_s$, with sides $a \times b = 400$ mm$\times$400 mm. Set the thickness of each composite layer to 0.2 mm and set $c = 100$ mm and $t_p = 0.1$ mm for all patches. Material properties are given in Table 1.

The analytical model employs an 8×8 finite element mesh and uses modal superposition techniques to test the effectiveness of actuators arranged in configurations A through D to suppress plate vibrations. The time interval is 0.005 s and patch feedback control gains are $G_v = 0.25$, and $G_d = 15$. Transient response determination is by Newmark-β integration setting $\alpha = 0.5$ and $\beta = 0.25$.

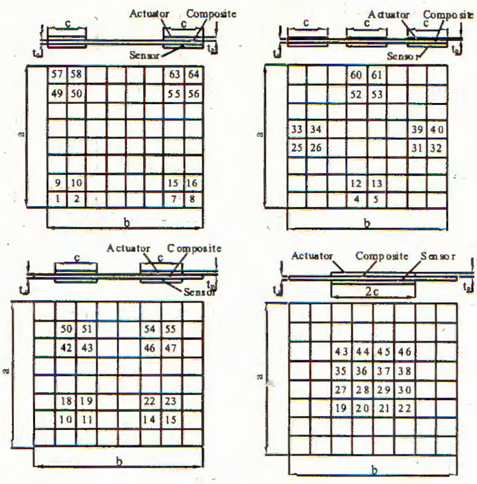

Fig. 6. Piezoelectric pair configurations

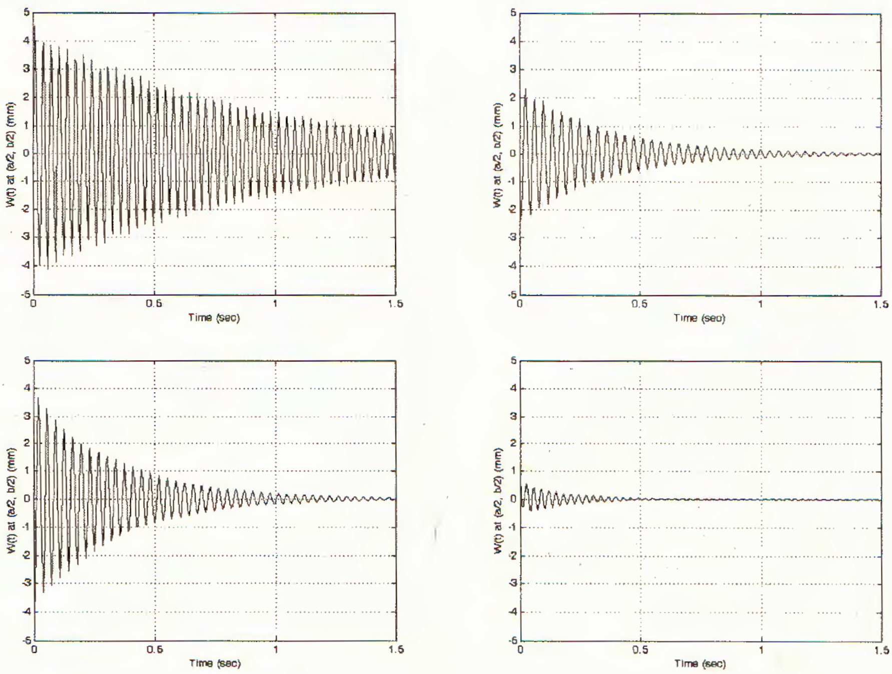

Fig. 7. Transient response of composite plates with integrated piezoelectric pairs

Fig. 7 compares the vibration control capabilities of the various configurations. Configuration D is clearly the most effective of these at limiting peak vibration amplitude and causing the rapid suppression of transient vibrations.

Table 3. Calculated natural frequencies (Hz)

Configuration	f_1	f_2	f_3	f_4	f_5
A	31.356	57.236	84.334	94.319	120.660
B	26.802	55.958	79.732	103.712	119.754
C	27.492	54.480	76.668	94.735	114.139
D	25.089	52.561	76.155	99.479	116.422

6. CONCLUSIONS

The FSDT based FE model can predict efficiently and accurately composite plates bonded or embedded with thin layers or piezoelectric sensors and actuators time dependent response to external load.

Active and passive voltage control methods are able to form and modify the shape, displacement profile and vibratory response of piezolaminated plates to static and time varying loads.

Stacking sequence, ply angle, and careful location of piezoelectric sensor/actuator pairs are all important factors needing careful consideration when designing optimum control systems. In particular:

Plate natural frequencies vary with sensor/actuator pair location.

Bonding sensor/actuator patches to plate centers promotes effective vibration suppression behavior.

This work is sponsored by the the Ministry of Science and Technology.

REFERENCES

1. Nguyen Dinh Thang, *Electric Materials (Courses of Lectures)*, Hanoi University of Technology.
2. D. T. Detwiler, M. H. H. Shen, V. B. Venkayya, Finite Element Analysis of laminated composite structures containing distributed piezoelectric actuators and sensors, *Finite Element in Analysis and Design* **20** (1995) 87-100.
3. A. Suleman and V. B. Venkayya, A simple finite element formulation for a laminated composite plate with piezoelectric layers, *Journal of Intelligent Material Systems and Structures* **6** (1995) 776-782.
4. D. B. Koconis, L. P. Kollar and G. S. Springer, Shape control of composite plates and shells with embedded actuators, *Journal of Composite Materials* **28** (1994) 415-458.
5. X. Q. Peng, K. Y. Lam and G. R. Liu, Active vibration control of composite beams with piezoelectric: a finite element model with third order theory, *Journal of Sound and Vibration* **209** (1998) 635-650.
6. D. A. Saravanos, P. R. Heyliger and D. A. Hopkins, Layerwise mechanics and finite element for the dynamics analysis of piezoelectric composite plates, *International Journal of Solids and Structures* **34** (1997) 359-378.
7. José M. Simões Moita, Cristóvão M. Mota Soares, Carlos A. Mota Soares, Geometrically non-linear analysis of composite structures with integrated piezoelectric sensors and actuators, *Composite Structures* **57** (2002) 253-261.

8. H. Fukunaga, N. Hu, G. X. Ren, FEM modeling of adaptive composite structures using a reduced higher-order plate theory via penalty functions, *International Journal of Solids and Structures* **38** (2001) 8735-8752.
9. G. R. Liu, X. Q. Peng and K. Y. Lam, Vibration Control Simulation of Laminated Composite Plates with Integrated Piezoelectrics, *Journal of Sound and Vibration* **220** (1999) (4) 827-846.
10. G. R. Liu, K. Y. Dai and K. M. Lim, Static and vibration control of composite laminates integrated with piezoelectric sensors and actuators using the radial point interpolation method, *Institute of Physics Publishing, Smart Mater. Struct* **13** (2004) 1438-1447.
11. José M. Simões Moita. "Geometrically non-linear analysis of composite structutes with integrated piezoelectric sensor and actuator". *Composite Structures* **57** (2002) 253-261.
12. G. L. C. M. De Abreu, J. F. Ribeiro and V. Jr. Steffen, Finite Element Modeling of a Plate with Localized piezoelectric Sensors and Actuators, *J. of the Braz. Soc. of Mech. Sci. & Eng. April-June 2004*, **26** (2) (2004).
13. Tran Ich Thinh, *Composite Materials - Mechanics of Materials and Structures*, Ed. Education, (1994), (In Vietnamese)
14. Tran Ich Thinh and Le Kim Ngoc, "Mechanical Analysis of Piezoelectric Composite Materials", *Proceedings of VIII-th National Conference on Mechanics of Deformable Solids*, Thai Nguyen, 2006, 814-825.

Received January 10, 2007

PHÂN TÍCH TĨNH VÀ ĐỘNG TẤM COMPOSITE ÁP ĐIỆN

Một mô hình phần tử hữu hạn được phát triển dựa vào lý thuyết tấm bậc nhất để điều khiển tĩnh và điều khiển dao động của tấm composite lớp có chứa các lớp hoặc miếng áp điện. Phần tử tứ giác đẳng tham số chín nút với 45 bậc tự do cơ học và 2 bậc tự do điện thế đã được xây dựng để phân tích tĩnh và động các tấm composite áp điện. Mô hình đã được kiểm tra qua so sánh kết quả với một số kết quả đã công bố. Qua kết quả số, có thể thấy rằng: bằng các điều khiển thụ động hoặc chủ động, ta có thể thu được hình dáng mong muốn cho tấm composite áp điện chịu tải trọng uốn. Ảnh hưởng của trật tự xếp các lớp composite, của vị trí các lớp áp điện và vị trí các cặp miếng cảm biến/kích thích được gắn vào tấm composite cũng được khảo sát và đánh giá.